CHAPTER 7 — FRONTS: CONCEPTUAL MODELS AND ANALYSIS; NON-FRONTAL SYSTEMS

CHAPTER 7 — FRONTS: CONCEPTUAL MODELS AND ANALYSIS; NON-FRONTAL SYSTEMS

7.1 Conceptual models — fronts and conveyor belts

Conceptual models provide the framework for the visualization and interpretation of satellite and radar imagery and are discussed in Bader et al., 1995, Chapters 4 & 5.

7.1.1 Fronts

At the most basic level a front represents the 'boundary between air masses of different thermal characteristics'. Frontogenesis is encouraged by: pressure falls on both sides of the front; convergence of two air streams; orographic influences (in particular a warm front, on approaching high ground, will intensify on the windward side). Conversely frontolysis will occur when there are pressure ~~falls~~ RISES on both sides of the front; there are divergent wind fields; and in the lee of high ground.

7.1.1.1 Ana- and kata-fronts

Warm fronts and cold fronts may have ana- or kata- characteristics depending on whether the warm air mass is rising up or subsiding down the frontal surface. A front may change from ana- to kata- at some point along its length, or at some time during its life history.

7.1.2 Conveyor belts; cyclogenetic models (Fig. 7.1)

Archetypal models are:

(i) Warm conveyor belts (ana- and kata-cold frontal situations, **Fig. 7.2**, **Fig. 7.3**, respectively).
(ii) Cold conveyor belts ahead of warm fronts.
(iii) Mesoscale rain bands — narrow and wide.
(iv) Other mid-latitude systems — comma clouds and cold-air vortices; polar trough conveyor belt and instant occlusions.

Bader et al. (1995), Chapters 4 and 5
Browning (1985)

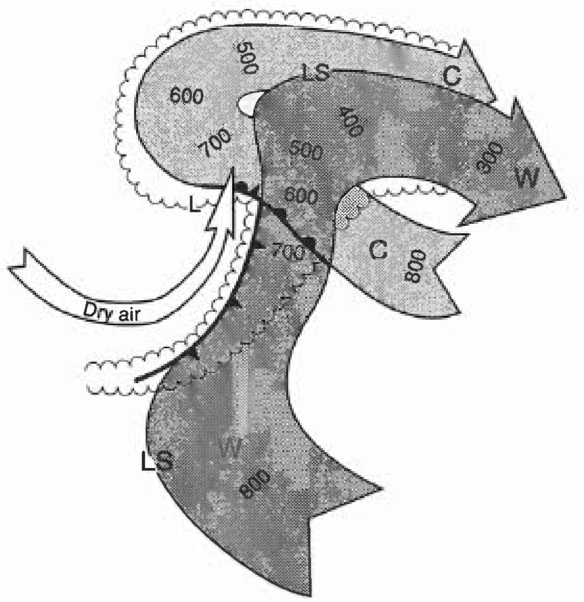

Figure 7.1. Model depicting the main features of the warm and cold conveyor belts in a mature mid-latitude depression. WW is the warm conveyor belt and CC is the cold conveyor belt. Figures within the broad arrows indicate the top of the belt in hectoPascals. The scalloped line represents the edge of the cloud produced by these flows. LS is the limiting streamline; L is the surface low.

7.1.3 The warm conveyor belt (WCB)

The dominant mechanism in frontal systems is baroclinic slantwise ascent in the form of a narrow airstream, the WCB, (**Fig. 7.1**) conveying large quantities of heat, moisture and westerly momentum. A small, but important, mainly ageostrophic, component perpendicular to the front produces two contrasting ascents: rearward and forward. Transitions from one to the other can occur along the front.

7.1.3.1 WCB with rearward-sloping ascent

This situation corresponds to the classical ana-front situation (**Fig. 7.2**); it is not as common in the UK as the forward-sloping one.

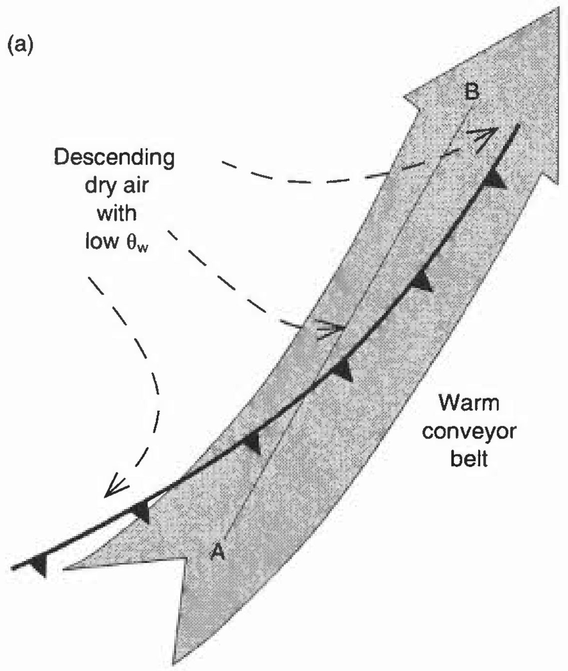

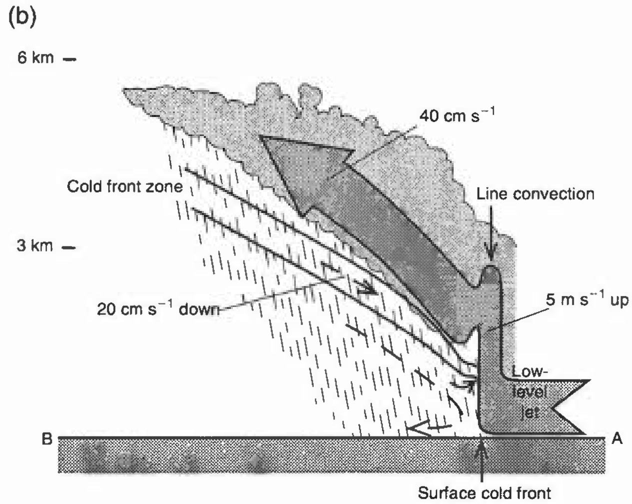

Figure 7.2. Schematic portrayal of airflow at a classical ana cold front showing the warm conveyor belt (bold arrow) undergoing rearward-sloping ascent above the cold-frontal zone with the cold air (dashed lines) descending beneath it: (a) plan view, (b) vertical section along AB in (a). LLJ marks the axis of the low-level jet. Flows are shown relative to the moving frontal system.

(i) The surface cold front tends to be sharp.
(ii) The warm boundary layer air ahead of the surface cold front is lifted abruptly some 2–3 km in a narrow strip adjacent to the cold front.
(iii) Further slantwise ascent above the cold air wedge produces two distinct precipitation patterns: a narrow band of very heavy rain at the surface cold front, and a broad belt of light-to-moderate rain behind, and often a little ahead of, the surface cold front.

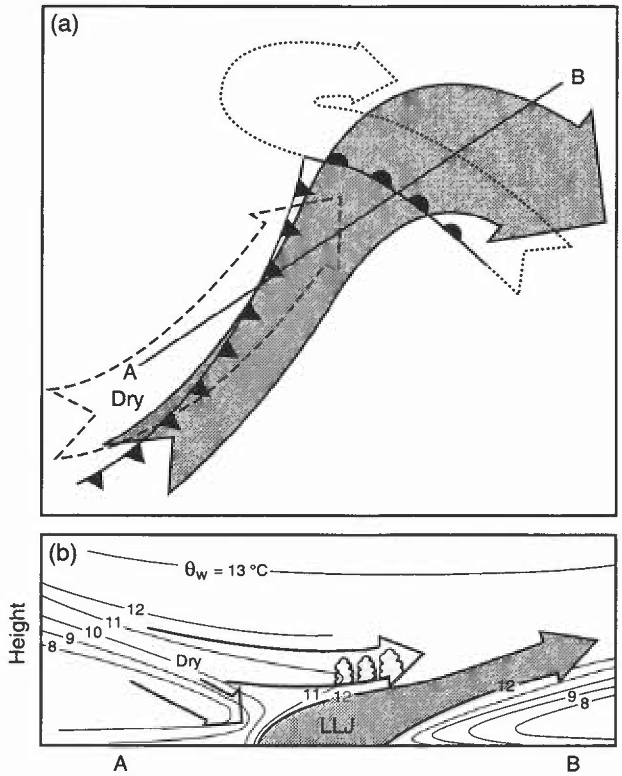

Figure 7.3. Schematic portrayal of airflow in a mid-latitude cyclone in which the warm conveyor belt (bold arrow with stippled shading) is undergoing forward-sloping ascent ahead of a kata cold front before rising above a flow of cold air ahead of the warm front (dotted arrow referred to as the cold conveyor belt). Cold middle-tropospheric air with low θ_w (dashed arrow) is shown overrunning the cold front and generating potential instability in the upper portion of the warm conveyor belt: (a) plan view, (b) vertical section along AB in (a). LLJ marks the axis of the low-level jet. Flows are shown relative to the moving frontal system.

7.1.3.2 WCB with forward-sloping ascent

This situation corresponds to the classical kata-cold front situation **(Fig. 7.3)**.

(i) Low θ_w air overruns the warm conveyor belt in mid-troposphere, leading to generation of potential instability, realized later as convection (in the UK it occurs more usually as shallow convection at middle levels).

(ii) The convex-poleward boundary to this flow where it ascends and turns to the right is often clearly detectable in satellite VIS imagery from the upper-cloud shadow cast on the lower cloud layer.

(iii) The leading edge of the overrunning dry, low θ_w, air often appears as a well-defined upper cold front **(Fig. 7.4)**; warm, moist air ahead, associated with organized convection, gives rise to a wide band of moderate-to-heavy rain.

(iv) The passage of the upper cold front is marked by scattered outbreaks of weakly convective rain. It may also be marked by a surface pressure trough or 'bar kick'. In general the upper cold front should be thought of as an upper wet-bulb temperature front; it is always accompanied by a decrease in humidity but not always accompanied by a significant decrease in dry-bulb temperature.

(iv) This is termed the 'split front' model because of the separate existence of the upper cold front; it is very common in the UK but can cause confusion if traditional classical frontal analysis is applied. The upper front should be identified distinctly.

Identification: compare the 700 hPa RH field with the position of the front as deduced from the 850 hPa chart; if the region of maximum RH lies forward of the frontal position, then this is likely to be a forward-sloping front.

Bader et al. (1995), Chapter 4
Browning (1995)

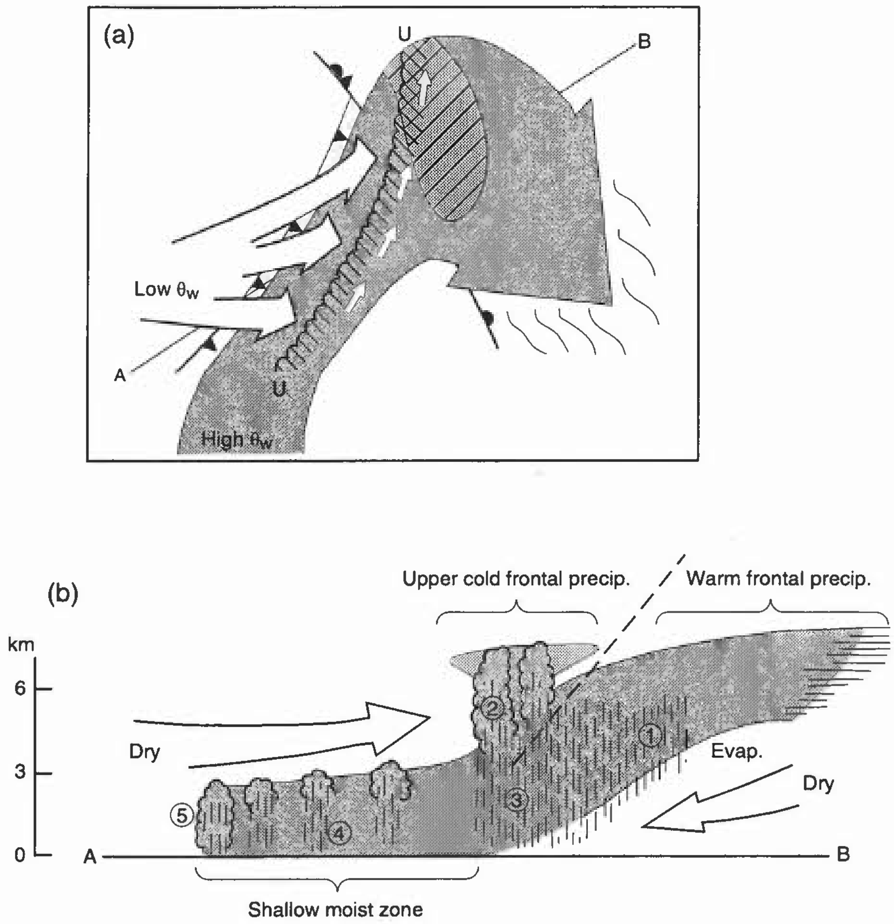

Figure 7.4. Schematic portrayal of the same situation as in Fig. 7.3, i.e. with the warm conveyor belt undergoing forward-sloping ascent, but drawing attention to the split-front characteristics and the overall precipitation distribution: (a) plan view, and (b) vertical section along AB in (a). In (a) UU represents the upper cold front. The hatched shading along UU and ahead of the warm front represents precipitation associated with the upper cold front and warm front, respectively. Numbers in (b) represent precipitation type as follows: 1, warm-frontal precipitation; 2, Convective precipitation-generating cells associated with the upper cold front; 3, precipitation from the upper cold-frontal convection descending through an area of warm advection; 4, shallow moist zone between the upper and surface cold fronts characterized by warm advection and scattered outbreaks of mainly light rain and drizzle; 5, shallow precipitation at the surface cold front itself.

7.1.4 The cold conveyor belt (CCB)

A secondary cloud-producing flow, the CCB, originates in the low-level flow to the north-east of a depression.

(i) Air in the CCB travels westwards, relatively, just ahead of the surface warm front beneath the WCB **(Figs 7.1 and 7.3)**.

(ii) Initially the air subsides and rain from the WCB, falling into it, evaporates. As it travels westwards towards the depression centre, it ascends, reaching into the middle troposphere near the apex of the warm sector.

(iii) Air near the surface warm front ascends due to frictional convergence; eventually the air may ascend slantwise out of the boundary layer into a cloud head, detectable in the satellite imagery, within which the rising air fans out, some of it ascending anticyclonically, and some of it descending cyclonically around the cyclone centre.

7.1.5 Slantwise convection and symmetric instability (2.9.10)

Motions resulting from the release of instability due to slantwise convection (symmetric instability), which can be regarded as a combination of buoyancy and ageostrophic forcing, may be responsible for, or important in:

(i) some of the detail observed in mesoscale precipitation bands;

(ii) the intense rearward ascent in ana-cold fronts;

(iii) the cloud head associated with explosive cyclogenesis.

Emanuel (1983) **Shutts (1990)**

7.1.6 Classification of mesoscale rain bands

To a first approximation, rain areas are aligned along the conveyor belt flows **(Figs 7.5 and 7.6)**. Sometimes the orientation is across the surface front when, for example, an upper cold front overruns the surface warm front. Precipitation is seldom uniform across a conveyor belt due to convective and mesoscale circulations:

(i) convection leads to groups of cells arranged in clusters, giving mesoscale precipitation areas tens of kilometres across;

(ii) The mesoscale circulations lead to banded precipitation structures which are sometimes quite uniform along their length, although more often they consist of aligned mesoscale areas.

Two principal categories of these mesoscale rain bands have been identified: narrow and wide.

7.1.6.1 Narrow rain bands

(i) The most significant occur in the cold seasons at the sharp surface cold frontal discontinuity in the situation of rearward-sloping ascent. These bands, seldom >3 km deep, are aligned along the surface front and frequently produce bursts of very heavy rain and sometimes hail **(Fig. 7.6)**.

(ii) The band of almost vertical convection, and the associated narrow cold-frontal rain band, is termed 'line convection' that can extend as an unbroken line for hundreds of kilometres, although it is more generally broken into line elements of tens of kilometres in length **(Fig. 7.7)**. Only when a full line element (as opposed to a 'gap') passes over will surface reports of transitions of temperature etc. give a realistic impression as to the nature of the front **(Fig. 7.8)**.

(iii) These rope-like cloud bands tend to occur towards the leading edge of the stratiform cloud generated by the slantwise convection. At the very edge they may be detectable by satellite imagery; although, even within the uniform stratiform mass the line convection will be clearly seen by radar.

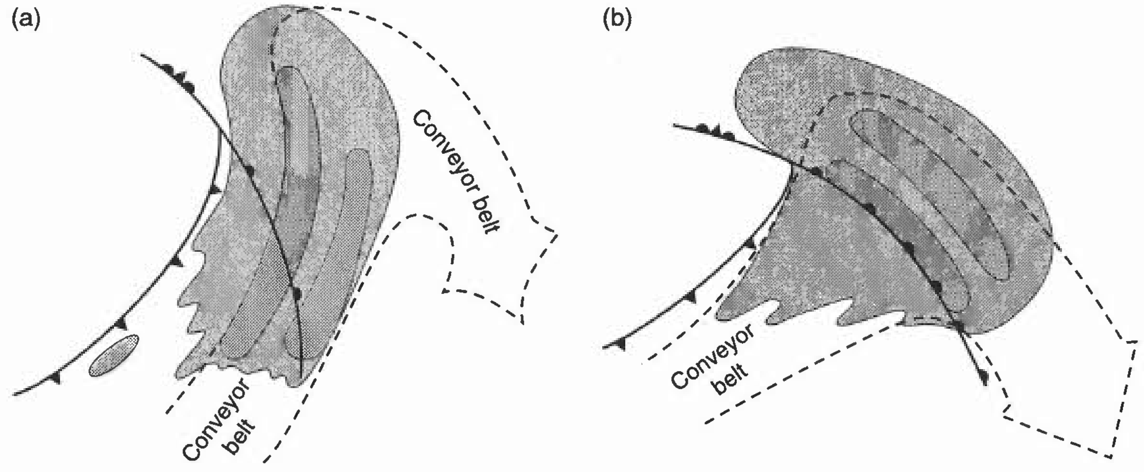

Figure 7.5. Rain areas associated with warm conveyor belts.

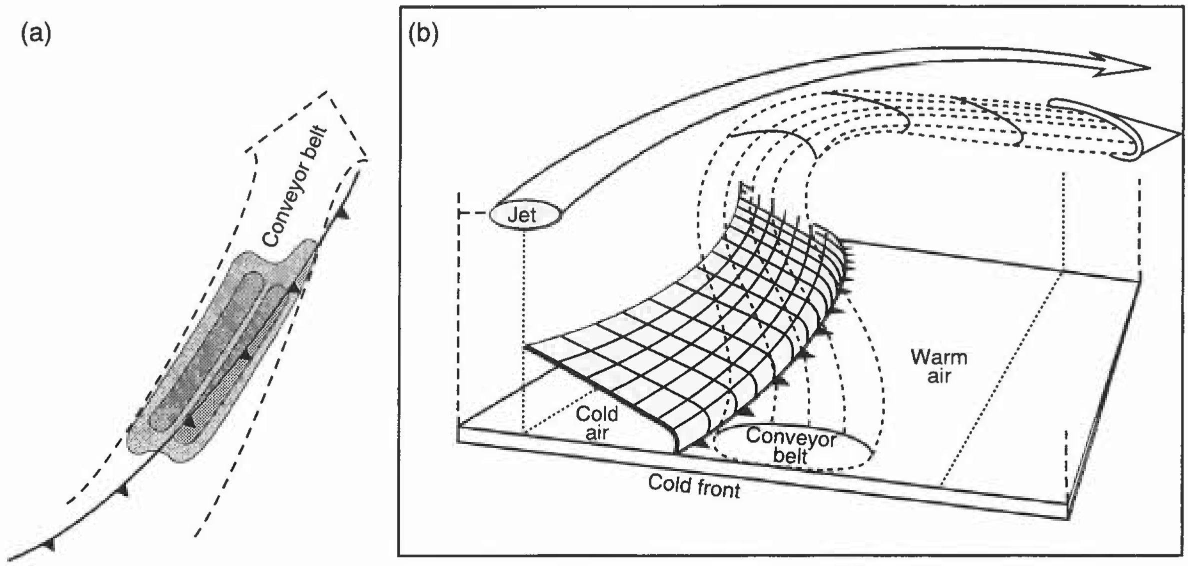

Figure 7.6. Conveyor belt ascending cold front: (a) plan view with rain areas, and (b) 3-D sketch with conveyor belt and jet stream.

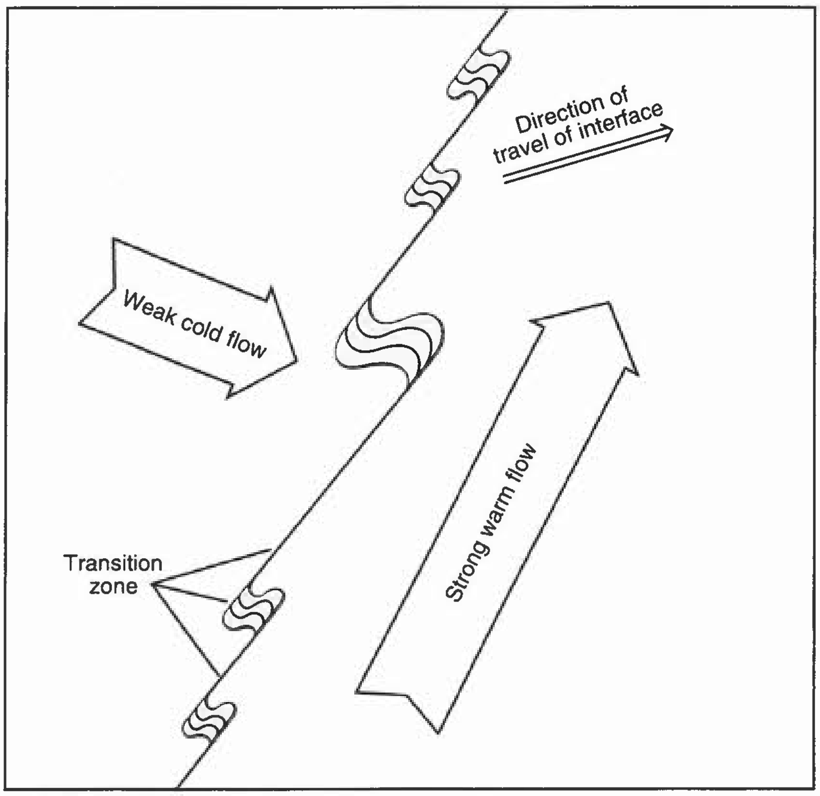

Figure 7.7. Schematic depiction of the transition zone at a sharp surface cold front. Line convection elements, with intense low-level convergence, strong updraughts and heavy precipitation, occur in the regions with a sharp transition zone. The regions where the temperature gradient is more gradual correspond to gaps between the line convection elements. The broad arrow, representing the flow at low levels on either side of the interface, are drawn relative to the ground.

7.1.6.2 Wide rain bands

There are several types: those in the warm sector are sometimes associated with squall lines, while post-frontal bands correspond to the cold-air comma clouds. The most common type is the upper-level rain band **(Fig. 7.5)**. These can occupy different positions within a frontal system, but can be considered as one dynamical type, the characteristics of which are:

(i) they are associated with the ascending parts of the WCB where its top reaches into the middle troposphere;
(ii) they may contain upper- or middle-level convective cells, often in clusters, which are generated within a shallow layer of potential instability where air with low θ_w overruns the WCB;
(iii) they are some 50 km wide and a few hundred kilometres long, orientated parallel to the baroclinicity at their level.

Bader et al. (1995), Chapter 4
Bradbury (1991), Chapter 3
Browning (1985)

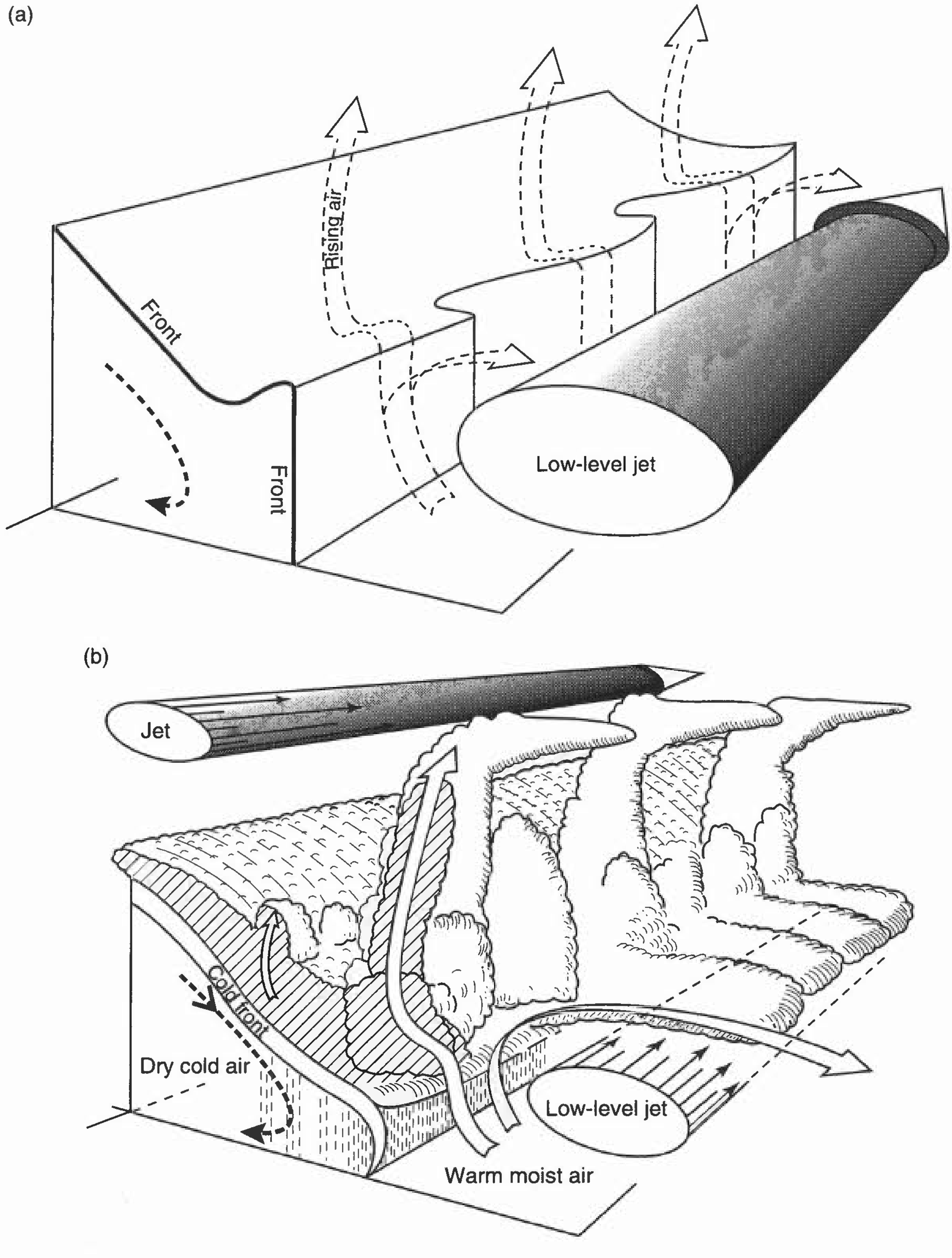

Figure 7.8. (a) Schematic 3-D structure of the cold front showing a low-level jet ahead of it, and (b) 3-D sketch of a cold front showing cloud, low- and high-level jets and patterns of air flow (after Bradbury (1991)).

7.1.7 Other mid-latitude systems

7.1.7.1 Sub-synoptic-scale comma clouds and cold-air vortices.

(i) Some phenomena classified as 'convective' can take on frontal characteristics, particularly evident in the comma-shaped cloud and sub-synoptic-scale precipitation systems associated with cold pools in polar air streams which develop most often over oceans in winter **(Fig. 7.9)**.

(ii) Baroclinicity and conditional instability coexist in the wide range of situations that occur — from conditional instability driving polar lows in very cold outbreaks over warm oceans to the case of comma-clouds due to baroclinic slantwise ascent, as in the short-wave polar troughs in westerlies behind major cold fronts approaching north-west Europe.

(iii) The comma cloud is characterized by convective precipitation and by a distinctive low-level jet as in the case of the synoptic-scale WCB.

(iv) When cloud from the preceding frontal system gets carried around the back of the cold pool (a bent-back, or wrap-around, occlusion) comma-clouds may develop from elements of this cloud as they travel around the southern flank of the pool **(Fig. 7.10)**.

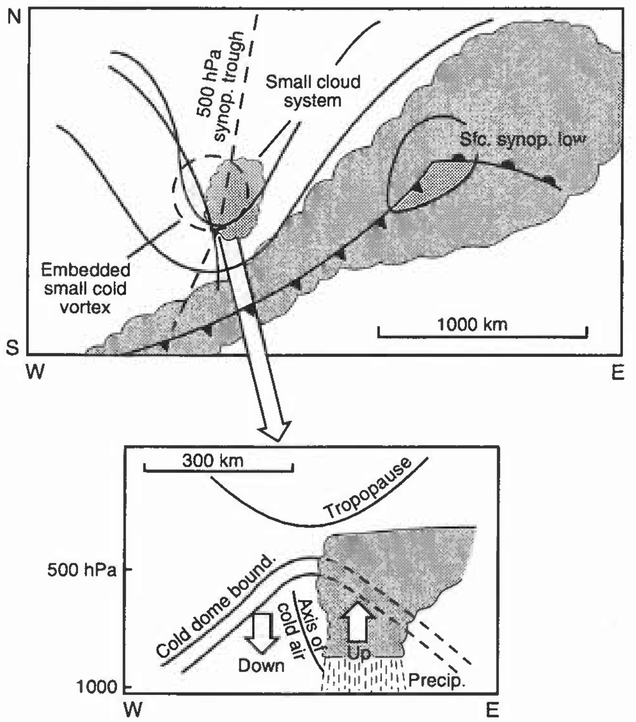

Figure 7.9. Schematic representation of a sub-synoptic-scale cold vortex.

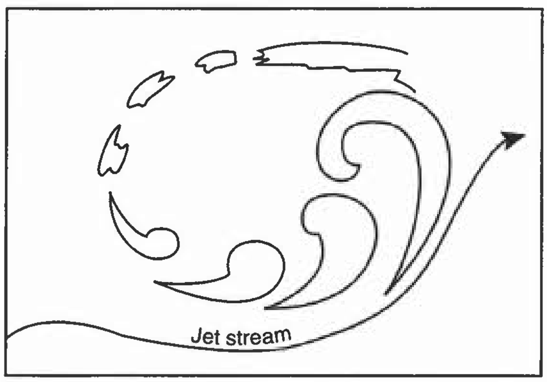

Figure 7.10. Schematic representation of successive stages in the life-cycle of a sub-synoptic-scale comma cloud as it travels around a cold pool behind an upper-level jet stream.

7.1.7.2 The polar trough conveyor belt and instant occlusion

(i) An instant occlusion is the name given to the lambda-shaped cloud pattern produced when a cloud band associated with a polar trough interacts with a cloud band associated with a polar front. The process is interpreted in terms of a dual conveyor belt configuration **(Fig. 7.11)**.

(ii) The instant occlusion is part of a spectrum of types **(Figs 7.12 and 7.13)** in which the form of the disturbance depends on the position of the short-wave trough or vorticity maximum with respect to the polar front.

(iii) The simple comma cloud development **(Fig. 7.12(a))** occurs well within the cold air, not interacting significantly with the main polar front **(Fig. 7.13(a))**.

(iv) By contrast, when the vorticity maximum is at the latitude of the polar front **(Fig. 7.12(c))**, a frontal wave forms in which the main WCB, associated with the polar front, gets involved in the circulation and dominates the cloud pattern **(Fig. 7.13(c))**.

(v) In the intermediate situation there are two distinct cloud belts, associated with the polar trough and polar front **(Figs 7.12(b) and 7.13(b))**.

Bader et al. (1995), Chapters 4 & 5 **Browning (1985)**
Bradbury (1991), Chapter 3

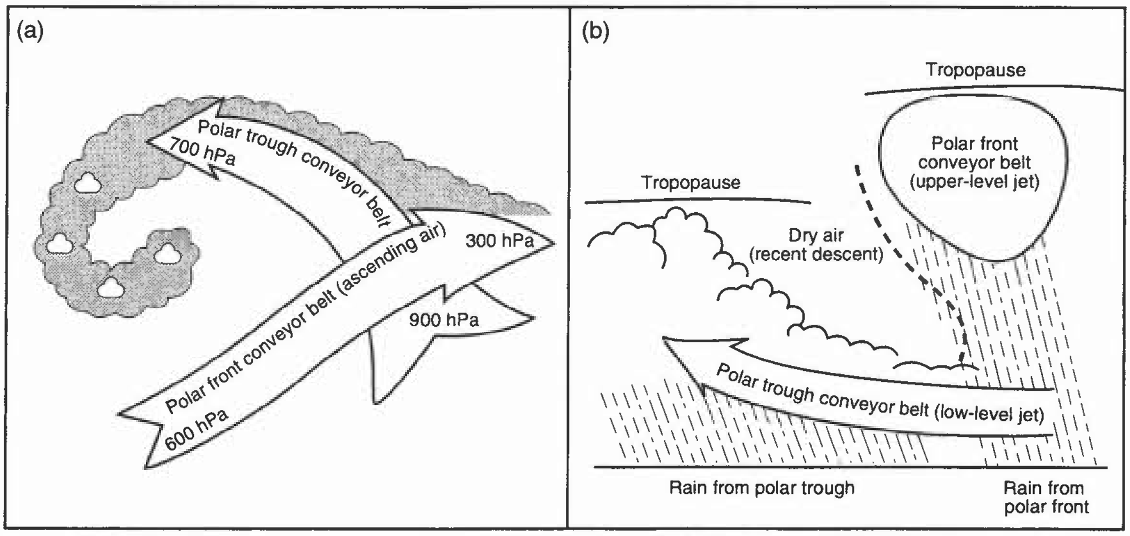

Figure 7.11. Schematic model of the lambda cloud system showing intersecting polar trough conveyor belt and polar front conveyor belt: (a) plan view, and (b) vertical section along axis of polar trough.

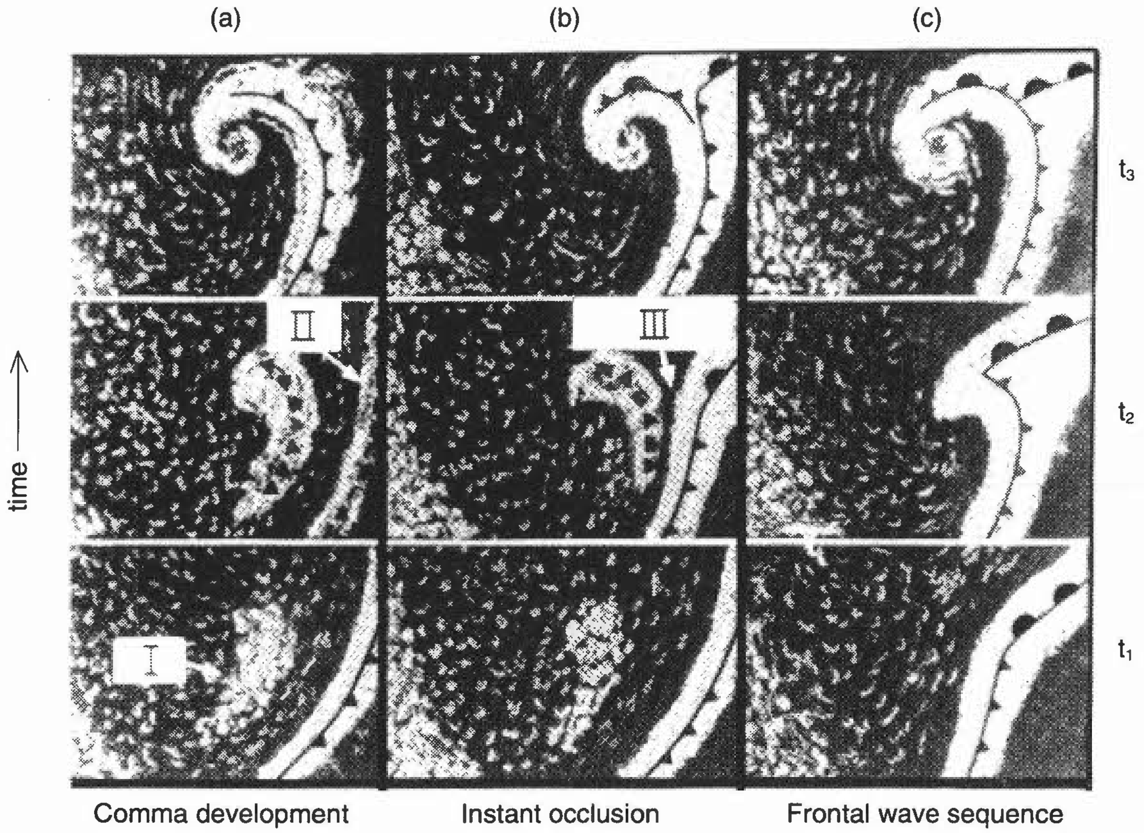

Figure 7.12. Schematic depiction of three basic sequences of vortex development evident in satellite imagery: (a) development of a comma cloud entirely within the cold air, (b) development of an instant occlusion, (c) development of a frontal wave. The figure was derived from observations over the Southern Ocean but it is printed vertically inverted so as to apply to the northern hemisphere. Frontal symbols indicate one scheme for representing the various evolution sequences using the tools of conventional frontal analysis. I, II and III, respectively, indicate a region of enhanced convection, a decaying cloud band and a convective cloud band merging with a frontal cloud band.

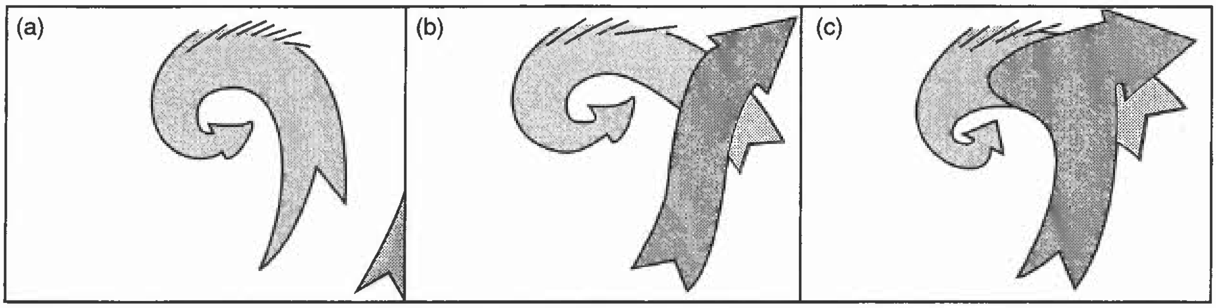

Figure 7.13. Schematic depiction of the conveyor belt flows associated with the cloud patterns at time t_1 in Fig. 7.12.

7.2 Frontal features and development

7.2.1 Features of a depression

Surface lows are usually associated with upper-level troughs; the trough line is not vertically above the surface low but displaced increasingly with height towards the region of coldest air. Upper ridges are similarly displaced from surface anticyclones.

In the lowest layers:

(i) Front lies on warm boundary of tightest θ_w gradient **(Fig. 7.14(a))**; a pronounced gradient of θ_w exists (Fig. 7.14c) near the surface cold front with decreasing θ_w with height (potential instability) at the bottom of the cold air mass. (Above 700 hPa, the pattern of the isentropes of ~~wet-bulb potential temperature~~ θ_w differ little from the pattern of ~~(Fig 7.14(b))~~ isentropes of θ).

(ii) A steeper (cold) frontal slope at low levels, with a tendency for the cold 'nose' to override surface front, means that 850 or 900 hPa position is similar to surface position **(Figs 7.14(b, c))**. However, shallow cold intrusions may travel >100 miles ahead of the 850 hPa θ_w.gradient, especially along an active front. Surface front often lies from half to two thirds into cloud band from cold side when seen from above. It may even be on the extreme warm side in certain cases.

7.2.2 Assessment of development of frontal depressions from synoptic charts

7.2.2.1 Empirical rules

Motion of surface pressure systems

Frontal depressions move, depending on state of development, as follows:

(i) If low or wave is *without a closed circulation and is not developing* it can be moved in the direction of the 1000–500 hPa thermal wind at about 1/2 the thermal wind speed or at 1/3 speed of the 300 hPa winds above the wave tip, in the 300 hPa direction.

(ii) *Open wave depressions, usually developing,* move at about 4/5 of the geostrophic speed in the warm air and in the corresponding direction or half the 500 hPa wind speed above the wave tip and in the corresponding direction.

(iii) The mature system moves in the direction of the warm sector isobars, with the speed of the 700 hPa flow.

(iv) A low may be moved parallel to a line joining the isallobaric high and low; there are no rules for quantifying the speed.

Intensity of surface pressure systems

(i) Frontal depressions deepen as markedly cold air is drawn into the rear of their circulation and as a warm anomaly in the lower stratosphere advances from the rear. Deepening is indicated by falls of pressure in the warm sector. Deepening may continue for 6–12 hours after the occlusion process starts.

(ii) Frontal depressions start to fill some 12–24 hours after the occlusion process begins; they slow and turn to the left. Pressure rises occur in the warm sector. Secondary depressions must be at least 600 n mile (1100 km) from the primary depression in order to deepen.

(iii) Over oceans the isallobaric pattern is often difficult to define because of the scarcity of observations and the effect of ships' motions on the observed pressure tendency.

Continuity is always a useful aid.

Bader et al. (1995), Chapters 4 & 5

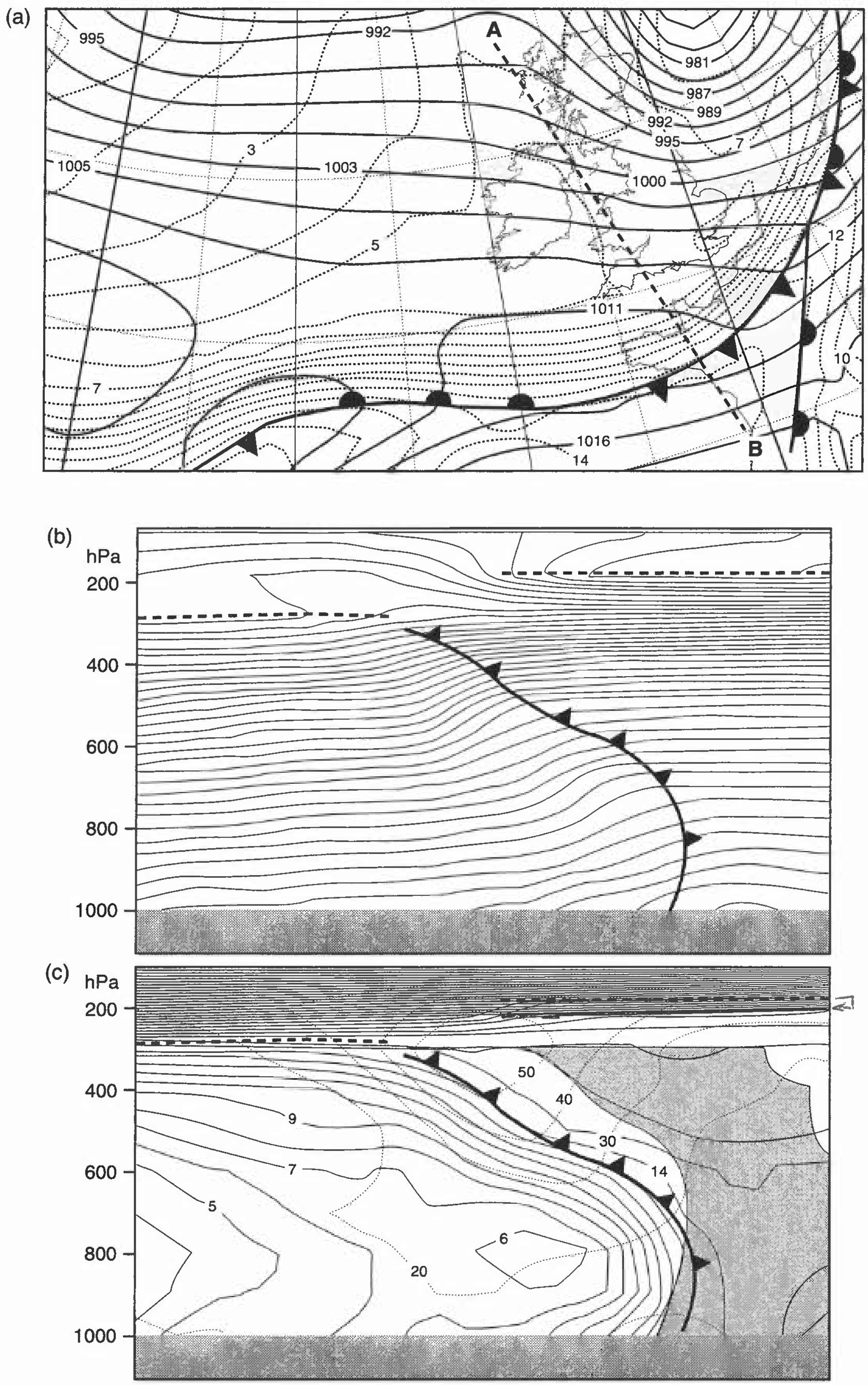

Figure 7.14. The structure of a cold front at 2100 UTC on 2 November 1992: 900 hPa WBPT every 1 °C (dotted), MSLP every 4 hPa (solid), (b) ~~potential~~ temperature (°C), and (c) cross-section through ana cold front (line AB in (a), distance 1400 km), solid lines represent WBPT every 1 °C, the shaded area frontal cloud, thin dashed lines the wind strength every 10 m s^{-1} and thick dashed lines the tropopause.

7.3 Explosive cyclogenesis (EC)

7.3.1 Definition

An explosively deepening depression is defined as a depression which deepens at a rate exceeding 24 hPa per day. Some such systems deepen at over twice that rate; falls of >10 hPa in 3 hours are often a precursor of EC.

7.3.2 Geographical and seasonal characteristics

(i) Explosive cyclogenesis (EC) is nearly always confined to oceanic regions, and predominantly occurs during the winter half of the year, with the western North Atlantic one of the world's most favoured areas.
(ii) However, EC can occur even in mid-summer and forecasters must be particularly alert to this possibility owing to the increased number of weather-sensitive activities at this time of year.
(iii) Explosively deepening depressions can develop from the remnants of ex-tropical storms in late summer and autumn.

7.3.3 Characteristic upper-air patterns

(i) The thickness gradient ahead of an upper trough interacting with a polar front is always intense prior to EC — typically 20 to 30 dam per 300 nautical miles.
(ii) A variety of upper-air patterns can lead to EC. By far the most favoured pattern is a short-wave trough or jet streak moving around a major mobile confluent trough. A general schematic of this type is shown in **Fig. 7.15**.
(iii) The importance of upper-level potential vorticity (PV) anomalies for cyclogenesis is well established.

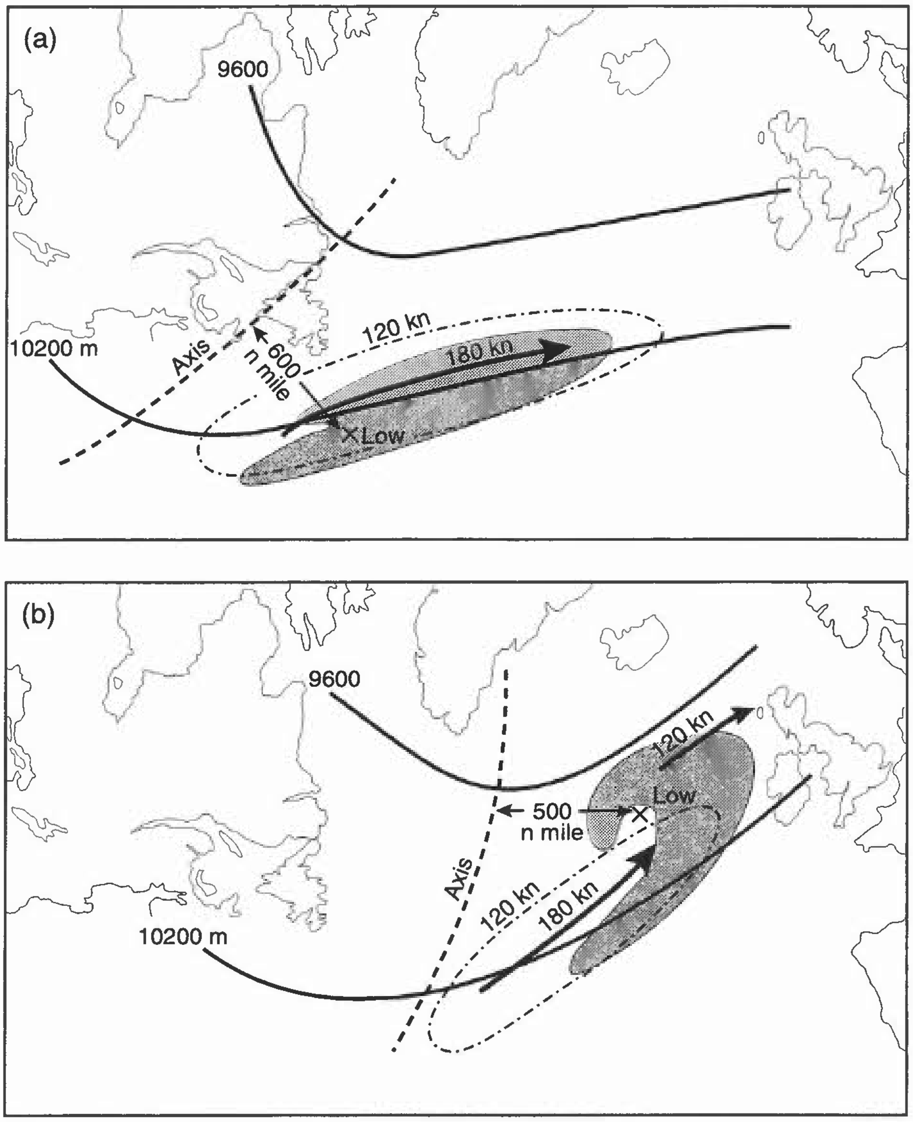

Figure 7.15. Schematic of low development ahead of a broad, mobile, confluent 250 hPa trough. Dispositions of surface centre relative to the 250 hPa pattern (a) at time of onset of rapid deepening, and (b) 24 hours later. Bold arrows are jet axes.

7.3.4 *Satellite imagery*

Damaging winds associated with EC are often preceded (by as much as 24 hours) by a 'cloud head', an example of which is shown in **Fig. 7.16**. This cloud head is characterized by:

(i) A very broad mass of dense layered cloud C, whose poleward edge often exhibits an 'S' shape. The cloud texture usually appears smooth on IR imagery, although VIS pictures in particular may show embedded convection arranged in transverse bands. Deep convection P in the adjacent polar air often undercuts C. The cloud head C is generated by the ascent and fanning out of air within the cold conveyor belt.

(ii) A narrow region, devoid of middle and upper cloud (but with significant sub-structure), known as the 'dry intrusion', which separates cloud head C from the adjacent band of frontal cloud F. The 'dry intrusion' consists of recently subsided air, partially stratospheric in origin, with high PV; when this air overruns a low-level baroclinic zone the effect of the overrunning high PV is to trigger cyclogenesis and ascent. Mesoscale events, including severe wind and precipitation, are closely related to the mesoscale PV maximum within the dry intrusion.

(iii) The surface depression centre is usually located within or close to the 'dry intrusion'. During deepening, the upstream tip of C evolves into a 'hook' around the surface low centre.

(iii) In addition, a rope-like cloud structure (line convection, 7.1.6.1) (often present at RR in **Fig. 7.16)** indicates the position of a new surface cold front (formally called the back-bent occlusion), which acquires the main low-level thermal gradient at the expense of the pre-existing front beneath F. Note: refer to recommended frontal analysis in Browning & Roberts (1994).

The above characteristic structures are not confined to explosive cyclogenesis.

Bader et al. (1995), Chapters 4 & 5
Browning et al. (1987)
Browning (1995)
Browning & Roberts (1994)
Monk & Bader (1988)
Norris & Young (1991)

7.3.5 *Winds associated with explosive cyclogenesis*

(i) Mean winds over the sea usually reach storm force, sometimes hurricane force, around a depression which has deepened explosively.

(ii) Early in the life-cycle, strongest winds are often found in the warm sector, but following explosive deepening, they occur near the hook of cloud as seen on satellite imagery, and are most likely just outside the southern edge of the hooked tip of the cloud head.

(iii) Rapid pressure rises to the rear of the depression centre in the cold air (sometimes exceeding 15 hPa in 3 hours) are a potent generator of damaging winds and are characteristic of lows developing ahead of a mobile confluent upper trough (and which is associated with the marked subsidence that typically occurs behind the confluent trough).

(iv) Such a pressure surge is not a feature of lows ahead of a major diffluent trough.

Young (1990)

7.3.6 *Precipitation*

Marked lowering of the freezing level (often by 1000 m) can occur in extensive heavy precipitation poleward of the depression centre, and rain may turn to snow over lowland areas when the 850 hPa wet-bulb potential temperature is 6° C or lower. Thunderstorms frequently occur at the boundary between the 'dry intrusion' and the hook of cloud late in the deepening phase.

7.3.7 *Factors mitigating against EC:*

(i) a rapidly relaxing upper trough;
(ii) the cloud head signature becoming ragged and ill-defined;
(iii) lack of warm air;
(iv) the depression centre moving from sea to land (possibly).

McCallum (1990)
McCallum & Norris (1990)

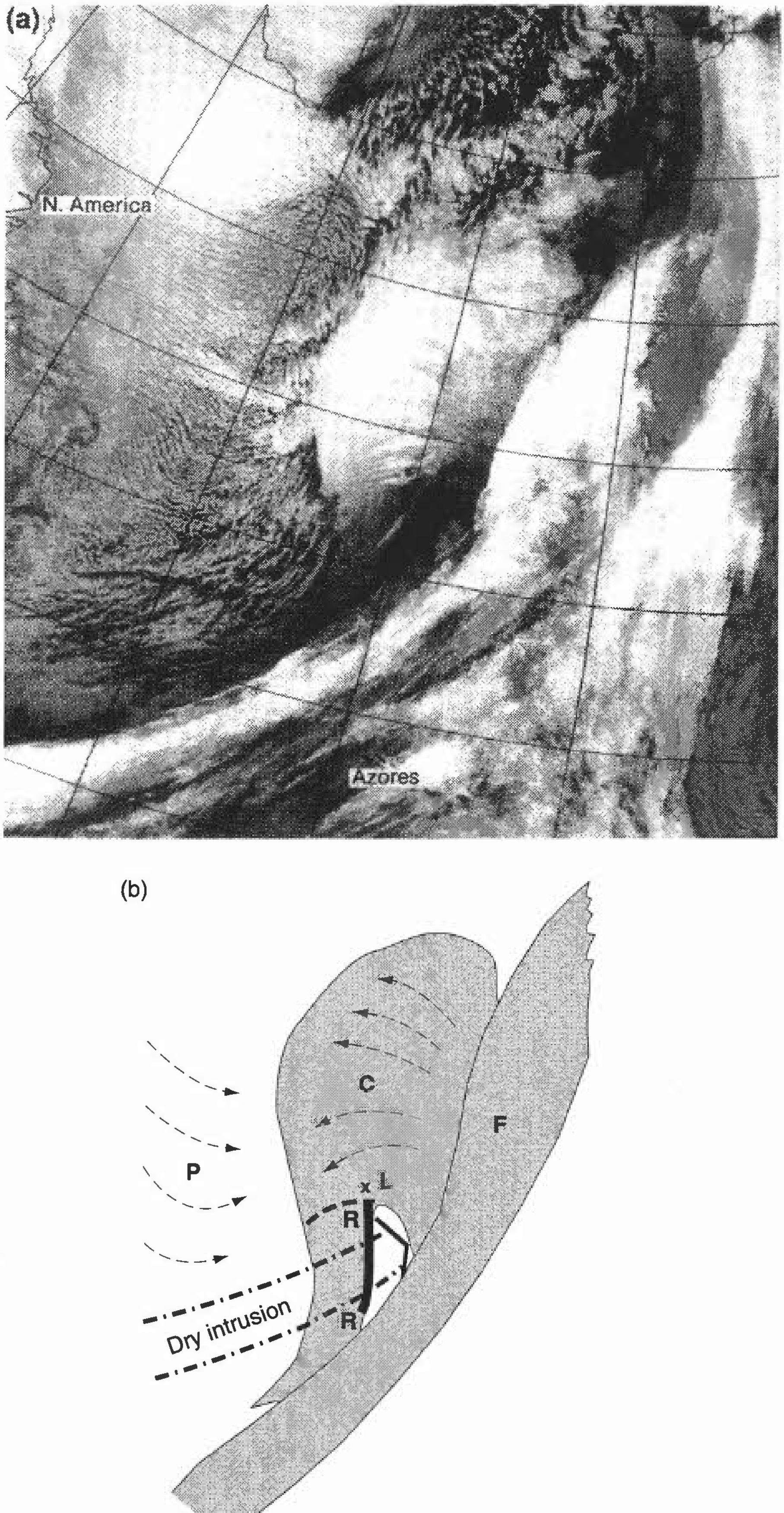

Figure 7.16. Infrared image showing cloud signature associated with early stages of EC at 1550 UTC on 2 February 1991, and (b) schematic diagram of the features described in the text.

7.4 Non-frontal systems

A number of other types of pressure system can affect the UK.

7.4.1 Old lows

(i) Circulation is present right through the depth of the troposphere; movement is slow and irregular.
(ii) It may be steered in the direction of strongest flow around it and cause other mobile features to be steered around it; sub-centres form and decay due to local convection.

7.4.2 Thermal lows

7.4.2.1 Heat lows

(i) Heat from warmed ground will extend up to, say, 850 hPa while temperature above is unaffected.
(ii) Surface pressure is therefore lower by a few hectopascals; in the UK the effect soon disappears as evening temperatures fall. Low-level convergence may trigger thunderstorms in unstable air.

7.4.2.2 Polar lows

(i) *Primary* lows develop as the result of the equatorward movement of an upper-level cold-cored vortex (or trough originating in a polar vortex region). Others are termed '*secondary*' (e.g. those forming as a by-product of normal extratropical cyclone development)
(ii) Comma clouds, waves on secondary baroclinic zones within the cold air mass, and lows that form on an occlusion are all examples of the latter type.
(iii) Sensible and latent heat input to polar lows will be continuous while over the sea; convective polar lows will usually decay rapidly after landfall.
(iv) Satellite imagery will reveal their presence in spite of their small scale (typically a few hundred kilometres in diameter).
(v) Low-level convergence, together with the strong pre-existing instability, often results in gale-force winds on the western flanks of, particularly, convective types and frequent showers or continuous precipitation resulting in significant accumulations of snow.

Significant parameter for development
Surface development is likely when a 500 hPa cold pool at −42 °C or below moves out over the open sea.

7.4.3 Orographic lows

Closed circulation lows in the lee of mountain ranges (as occurs in the Alps) are not common in the UK, though lee troughing is often observed. Lee lows frequently form to the lee of the Greenland plateau where they may alter the large-scale synoptic development of systems in the North Atlantic.

7.4.4 Old tropical depressions

Occasionally, generally in autumn, decaying tropical depressions, with very warm, moist air within their circulations, get caught up and reinvigorated in the mid-latitude westerly flow, feeding off baroclinic instability. They reach the UK as vigorous depressions giving strong winds and copious rain.

7.4.5 Summary of movement and development indicators

Non-frontal depressions move:
(i) with the strongest winds around their periphery;
(ii) around the circulation of a larger primary depression;
(iii) as a rotating system ('dumb-bell') if two (or more) equal sized lows are present. Detailed movement is difficult to forecast.

The best indicators of their development are the observed pressure tendencies.

7.4.6 Anticyclones

High pressure areas can be clear or cloudy, presenting a difficult forecasting problem for St or Sc, particularly in winter. Generally, highs will build if warm air is advected northwards on their western flank and cold air is advected southwards on their eastern flank, declining when encircled by warm air. They will move towards regions of rising pressure.

7.4.6.1 Cold anticyclones

In one type cold, dense air is confined to the lower troposphere following protracted radiation cooling over large land masses such as Canada or Siberia during winter. Another type forms between two successive depressions, but is mobile, moving with speed similar to the depressions; it is steered parallel to thickness lines.

7.4.6.2 Warm anticyclones

In this system cold, dense air is largely confined to the upper troposphere and lower stratosphere, the middle and lower troposphere often being warmer than usual. The subtropical anticyclones, such as the Azores high, are of this type. The highest MSLPs arise from cold air at low levels, exceptionally, combining with a higher-than-average tropopause.

7.4.6.3 Blocking highs

Anticyclones centred between 50 and 70° N prevent the polar front from occupying its normal position, thus blocking the progress of frontal depressions. There is a tendency for blocking highs to persist in preferred geographical areas, especially between 10 and 20° W, just to the west of the UK, and between 10 and 20° E, over Scandinavia.

7.4.7 Other synoptic features

(i) A *trough of low pressure* may occur simply as an extension of a low pressure area, or as a sharper, more well-defined feature, such as is found across a front of occasionally in unstable polar air.

(ii) A well-marked trough is often marked by lines of enhanced convection and, occasionally, by persistent rain. It will move with the component of the geostrophic wind speed across it.

(iii) The weather in a *col* tends to be calm, but diffluence in the larger-scale flow around a col can lead to frontogenesis.

Bader et al. (1995), Chapter 5
HWF (1975), Chapter 6.3

BIBLIOGRAPHY

CHAPTER 7 — FRONTS: CONCEPTUAL MODELS AND ANALYSIS; NON-FRONTAL SYSTEMS

Bader, M.J., Forbes, G.S., Grant, J.R., Lilley, R.B.E. and Waters, J., 1995: Images in weather forecasting. Cambridge University Press.

Bradbury, T.A.M., 1991: Meteorology and flight. A.C. Black.

Browning, K.A., 1985: Conceptual models of precipitation systems. *Meteorol Mag*, **114**, 293–318 (includes list of other definitive papers).

Browning, K.A., 1995: Mesoscale aspects of extratropical cyclones: an observational perspective. Joint Centre for Mesoscale Meteorology, Internal Report No. 44.

Browning, K.A., Bader, M.J., Waters, A.J., Young, M.V. and Monk, G.A., 1987: Applications of satellite imagery in nowcasting severe storms and very short range forecasts. *Meteorol Mag*, **116**, 161–179.

Browning, K.A. and Golding, B.W., 1995: Mesoscale aspects of a dry intrusion within a vigorous cyclone. *QJR Meteorol Soc*, **121**, 463–495.

Browning, K.A. and Roberts, N.M., 1994: Structure of a frontal cyclone. *QJR Meteorol Soc,* **120**, 1535–1557.

Emanuel. K., 1983: On assessing local conditional symmetric instability from atmospheric soundings. *Mon Weather Rev*, **111**, 2016–2033.

McCallum, E., 1990: The Burns' Day storm, 25 January 1990. *Weather*, **45**, 166–173.

McCallum, E. and Norris, W.J.T., 1990: The storms of January and February 1990. *Meteorol Mag*, **119**, 201–210.

Monk, G.A. and Bader, M.J., 1988: Satellite images showing the development of the storm of 15–16 October 1987. *Weather*, **43**, 130–135.

Norris, W.J.T. and Young, M.V., 1991: Satellite photographs — 2 February 1991 at 1533 UTC. *Meteorol Mag*, **120,** 115–116.

Orographic Processes in Meteorology (Pre-prints), 1993: Summer School, Meteorological Office College, Shinfield.

Shutts, G.J., 1990: SCAPE charts from NWP model fields. *Mon Weather Rev*, **118**, 2745–2751.

Young, M.V., 1990: Satellite and radar images, 0900 GMT 3 February 1990. *Weather*, **45**, 268–270.